Available online at www.sciencedirect.com
ScienceDirect
Journal of Solid State Chemistry 180 (2007) 1390–1396
JOURNAL OF SOLID STATE CHEMISTRY
www.elsevier.com/locate/jssc

Controlled synthesis of CuO nanostructures by a simple solution route

Zeheng Yang, Jun Xu, Weixin Zhang*, Anping Liu, Shupei Tang

School of Chemical Engineering, Hefei University of Technology, Hefei, Anhui 230009, PR China

Received 21 November 2006; received in revised form 7 February 2007; accepted 11 February 2007
Available online 22 February 2007

Abstract

A simple solution route has been developed to prepare nanostructured CuO with $Cu(NO_3)_2 \cdot 3H_2O$ and NaOH as starting materials. CuO nanoribbons or nanorods and their assemblies into hierarchical structures have been synthesized, respectively, by controlling the molar ratio of NaOH to $Cu(NO_3)_2$, reaction temperature and the concentration of the starting NaOH solution. Experiments demonstrate that the molar ratio of NaOH to $Cu(NO_3)_2$ is an important parameter which may decide whether CuO exists in nanoribbons (nanorods) or assemblies into hierarchical structures. Whether $Cu(NO_3)_2$ is dissolved in ethanol or water also influences the formation of monodispersed CuO nanoribbons (nanorods). The growth mechanism of these nanostructures is discussed. The products were characterized by X-ray diffraction, field-emission scanning electron microscopy and transmission electron microscopy (HRTEM) and their optical absorption spectra were also studied.

Keywords: Synthesis; Nanostructures; Copper oxide; Solution route

1. Introduction

As a p-type semiconductor with a narrow band gap ($E_g = 1.2$ eV) [1], CuO is a unique monoxide compound (in monoclinic phase, different from normal rock-salt type structure) for both fundamental investigations and practical applications. CuO has been used as heterogeneous catalysts in many important chemical processes, such as degradation of nitrous oxide, selective catalytic reduction of nitric oxide with ammonia, and oxidation of carbon monoxide, hydrocarbon and phenol in supercritical water [2–4]. Recent studies found that CuO could exist in as many as three different magnetic phases and form the basis for several high-T_c superconductors and materials with giant magnetoresistance [1,5–8]. CuO can be also used as gas sensors [9,10], optical switch [11], magnetic storage media [12], lithium batteries [13,14] and solar cells [15,16] owing to its photoconductive and photochemical properties.

Nanoscaled materials are of great interest due to their unique optical, electrical and magnetic properties and their potential applications in nanodevices [17,18]. As we know, these properties of nanomaterials are highly size- and shape dependent [19], and therefore it is extremely important to be able to properly control the size and morphology of the nanomaterials.

In recent years, nanostructured CuO materials and assemblies have attracted considerable attention due to its fundamental and practical importance [20–27]. Hu and co-workers have synthesized CuO nanotubes and nanorods by hydrothermal treatment of $[Cu(OH)_4]^{2-}$ in the presence of CTAB [20]. Xia and co-workers reported the synthesis of CuO nanowires by heating copper substrates in air within the temperature range of 400–700 °C [21]. CuO nanorods, nanoribbons and dandelion-like hollow microspheres have been fabricated in water–ethanol mixed solvent by Huachun Zeng's group [22,23]. Chen and co-workers have prepared pricky CuO microspheres by a solvothermal route [24]. Li and co-workers have used monodispersed Cu_2O nanospheres as precursors to synthesize CuO nanospheres by gas-phase oxidation [10]. Recently, we have successfully fabricated CuO nanotube arrays and nanoflower films on copper foil, respectively [25]. However, it is still a challenge for us to prepare a variety of CuO nanostructures and their assemblies in the same reaction system only by manipulating reaction conditions.

*Corresponding author. Fax: +86 551 290 1450.
E-mail address: wxzhang@hfut.edu.cn (W. Zhang).

0022-4596/$ - see front matter © 2007 Elsevier Inc. All rights reserved.
doi:10.1016/j.jssc.2007.02.008

In this work, we report a simple solution route to prepare various CuO nanostructures, including nanoribbons or nanorods and their spherical or flower-like hierarchical assemblies. The morphology of these CuO nanostructures can be effectively controlled by manipulating reaction conditions such as the molar ratio of NaOH to $Cu(NO_3)_2$, reaction temperature and the concentration of the starting solution. A possible illustration of the effect of ethanol on the morphology of CuO nanostructure is proposed. Our research results further enrich the hierarchical CuO architecture family.

2. Experimental

All the reagents were of analytical grade and were used without further purification. Stock solution of NaOH was prepared by dissolving NaOH in distilled water and $Cu(NO_3)_2$ solution was prepared by dissolving $Cu(NO_3)_2 \cdot 3H_2O$ in absolute ethanol solvent. Six synthetic schemes (A1–A3, and B1–B3) were devised in the present experiments. The detailed preparation procedures and conditions are summarized in Table 1. For A1, B1 and B2, the solution mixture was transferred into a Teflon-lined stainless steel autoclave of 50 mL capacity which was then heated at 100 °C for a given time. After reaction, the autoclave was cooled in tap water. For A2, A3 and B3, the reaction was conducted in a beaker at 50 °C or room temperature. The resultant precipitates were washed with distilled water and ethanol, respectively. Finally, the products were dried in vacuum at 60 °C for 12 h.

The as-prepared samples were characterized by X-ray powder diffraction (XRD) in a Rigaku D/max-γ B X-ray diffractometer with a Cu$K\alpha$ radiation source ($\lambda = 1.5418$ Å) operating at 40 kV and 80 mA. Field-emission scanning electron microscopy (FE-SEM) measurement was taken by JEOL 7500B scanning electron microscopes. A thin film of gold was sputtered on the sample surface to prevent charging. Transmission electron microscopic (TEM) images were taken with Hitachi H-800 and high-resolution transmission electron microscopic (HRTEM) images were taken with JEOL-2010 transmission electron microscope performed at an accelerating voltage of 200 kV. UV–vis absorption spectra were recorded on an UV2550 spectrophotometer.

3. Results and discussion

In Fig. 1, typical XRD patterns for the sample series are displayed. The major peaks located at 2θ values of 30–70° correspond to the characteristic diffractions of monoclinic phase CuO (JCPDS 48-1548), indicating that all the products are phase-pure. With the reaction temperature increases, the diffraction peaks show stronger intensity and

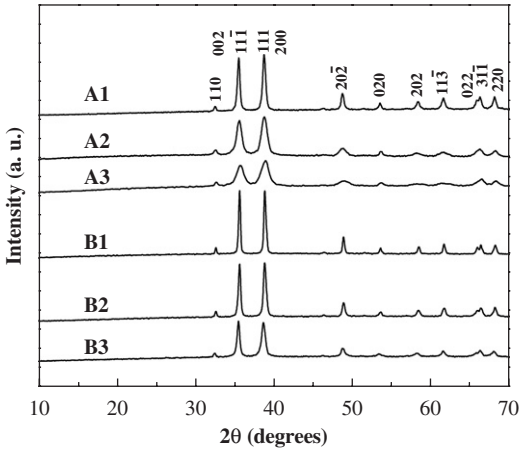

Fig. 1. The XRD patterns of the sample series of A1–A3, and B1–B3.

Table 1
Experimental procedures and products

	Preparation procedure	The molar ratio of NaOH to $Cu(NO_3)_2$	Results
Experiment A			
1	10.0 mL of NaOH (10.0 M) + 5.0 mL of $Cu(NO_3)_2$ (0.50 M), 100 °C, aged for 12 h, in autoclave	40	CuO nanorods (length less than 1 μm, breadth = 50–100 nm, straight)
2	10.0 mL of NaOH (10.0 M) + 5.0 mL of $Cu(NO_3)_2$ (0.50 M), 50 °C, aged for 12 h, in beaker		CuO nanoribbons (length more than 1 μm, breadth = 30–50 nm, curved)
3	10.0 mL of NaOH (10.0 M) + 5.0 mL of $Cu(NO_3)_2$ (0.50 M), room temperature, aged for 26 h, in beaker		CuO nanoribbons (length less than 1 μm, breadth = 15–30 nm, curved)
Experiment B			
1	10.0 mL of NaOH (10.0 M) + 1.0 mL of $Cu(NO_3)_2$ (0.50 M) at 0.5 mL min^{-1}, 100 °C, aged for 24 h, in autoclave	200	CuO flower-like assembly (building block: dozens of CuO nanorods of 1.5–2 μm in length with cuspate tips, straight, loosely)
2	20.0 mL of NaOH (5.0 M) + 1.0 mL of $Cu(NO_3)_2$ (0.50 M) at 0.5 mL min^{-1}, 100 °C, aged for 24 h, in autoclave		CuO spherical assembly (building block: hundreds of CuO nanorods of 1–2 μm in length with aclinic tips, straight, compactly)
3	20.0 mL of NaOH (5.0 M) + 1.0 mL of $Cu(NO_3)_2$ (0.50 M) at 0.5 mL min^{-1}, room temperature, aged for 72 h, in beaker		CuO spherical assembly (building block: hundreds of CuO nanoribbons of 0.5–1 μm in length, curved, compactly)

narrower width, which indicate that higher temperature improves the crystallinity of the products.

For the sample series of A, the molar ratio of NaOH to $Cu(NO_3)_2$ was 40 as shown in Table 1. Their typical TEM images (Fig. 2) indicate that all the three samples show one-dimensional (1D) morphology. But their crystal size and structures are different actually. Sample A1 was prepared in autoclave at 100 °C and thus it is well crystallized. The obtained CuO nanorods (Fig. 2a) have a length less than 1 μm, and the breadth ranges from 50 to 100 nm. The nanorods are very thin and monodispersed. The corresponding ED pattern along the [0 0 1] zone axis of the CuO nanorod (Fig. 2d) indicates that it is single crystalline. In fact, similar ED patterns can also be observed on different parts of the same nanorod. When the reaction temperature falls to 50 °C for sample A2, CuO nanoribbons with lengths more than 1 μm can be obtained as shown in Fig. 2b. The breadths of the as-prepared CuO nanoribbons can be decreased to the ranges of 30–50 nm. The related ED pattern (Fig. 2e) indicates that the CuO nanoribbons prepared at 50 °C are actually polycrystalline. When the reaction temperature is further decreased to room temperature (about 25 °C) for sample A3, as shown in Fig. 2c, the breadth of the CuO nanoribbons can be significantly decreased to the ranges of 15–30 nm. The corresponding ED pattern in Fig. 2f shows that these nanoribbons are also polycrystalline.

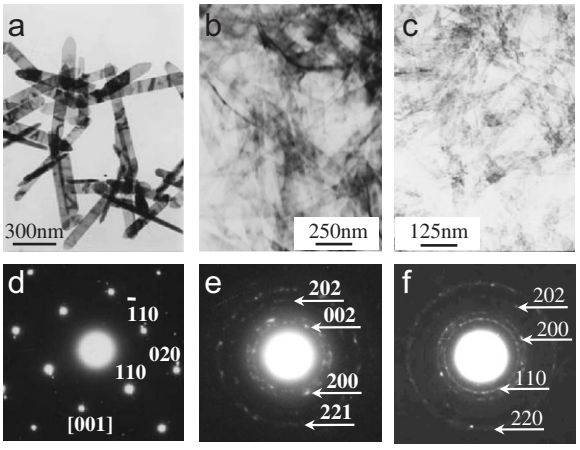

Fig. 2. TEM images and their corresponding ED patterns for samples A1 (a, d), A2 (b, e) and A3 (c, f).

For the sample series of B, the molar ratio of NaOH to $Cu(NO_3)_2$ was raised to 200 as shown in Table 1. Their typical TEM images (Figs. 3–5) indicate that all the three samples have a sphere-like or flower-like morphology. But there exist differences among their crystal size and structures.

Compared with sample A1, sample B1 was prepared with 1.0 mL of $Cu(NO_3)_2$ (0.50 M) instead of 5.0 mL and accordingly the molar ratio of NaOH to $Cu(NO_3)_2$ was increased to 200, with other reaction conditions unchanged. The FE-SEM images (Fig. 3a) show that sample B1 consists of CuO microflowers on large scale and each flower has a size of 3–4 μm. These uniform flower-like assemblies are made up of dozens of loosely compacted thin CuO nanorods of 1.5–2 μm in length and 500–800 nm in width with cuspate tips (Fig. 3b and c). The SAED pattern (Fig. 3d) of the nanorod along the [0 0 1] zone axis indicates that the CuO petal is a single crystal, which is corroborated by the HRTEM image in Fig. 3e. The fringe of the planes (1 1 0) is 0.278 nm and the fringe of the planes ($\bar{1}$ 1 0) is 0.269 nm.

Compared with sample B1, sample B2 was prepared under lower concentration (5.0 M) of NaOH, but the molar

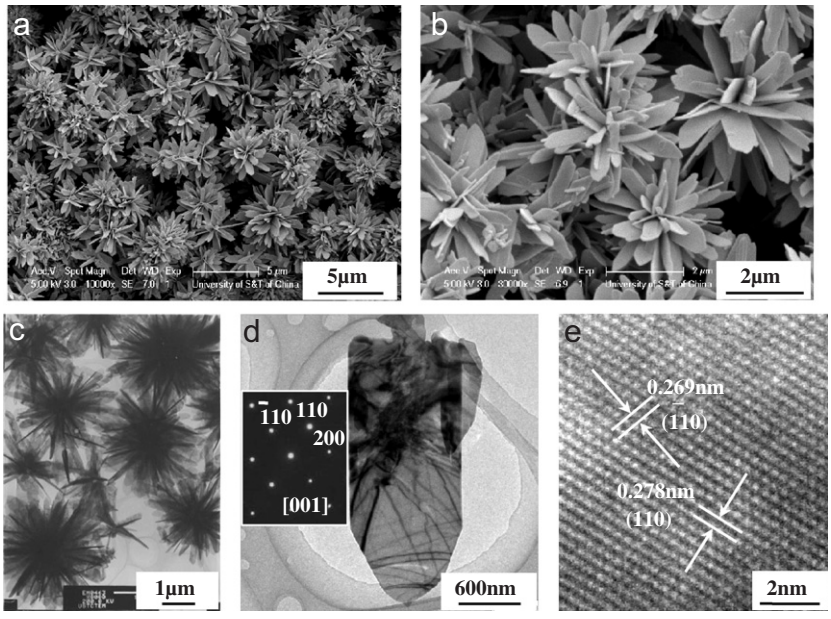

Fig. 3. FE-SEM (a, b) and TEM (c) images of flower-like CuO assemblies corresponding to sample B1; TEM (d) and HRTEM (e) images of a single CuO nanorod in it. *Inset of part (d)*: SAED pattern of the single CuO nanorod.

quantities of NaOH and other reaction conditions were the same. In this case, large-scale monodispersed CuO microspheres are observed under FE-SEM (Fig. 4a). The diameter of the CuO microspheres is in the range of 2–3 μm (Fig. 4b), a bit smaller than that of sample B1. The magnified FE-SEM image (inset in Fig. 4a) and TEM image (Fig. 4c) show that compared with sample B1, the morphology of sample B2 is greatly changed. The CuO microspheres in sample B2 are made up of hundreds of compactly self-assembled nanorods with the breadths of 50–400 nm and lengths of 1–2 μm. All these nanorods have aclinic tips. These CuO microspheres (sample B2) have more petals than the CuO microflowers (sample B1). The HRTEM image (Fig. 4d) of a nanorod shows a lattice fringe with a constant spacing of 0.27 nm corresponding to that of the (1 1 0) planes of CuO. The inset SAED pattern indicates that the CuO nanorod is single crystalline.

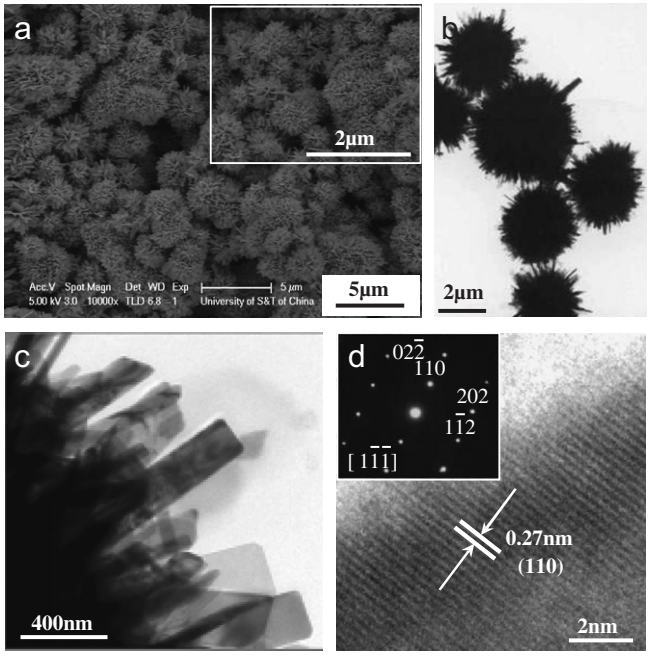

Fig. 4. FE-SEM (a) and TEM (b, c) images of spherical CuO assemblies corresponding to sample B2; HRTEM (d) images of a single CuO nanorod in it. Inset of part (a): a higher magnification FE-SEM image of a single CuO microsphere; inset of part (d): SAED pattern of the single CuO nanorod.

Sample B3 was prepared at room temperature under atmosphere and other reaction conditions were the same as those for sample B2. Fig. 5a shows that it is made up of many agglomerates. The TEM images (Fig. 5b and c) indicate that the agglomerates are spherical assemblies with diameters of 1–2 μm, which are a bit smaller than that of sample B2 due to lower reaction temperature. The magnified TEM image shown in Fig. 5d indicates that the microsphere is built from 1D curved nanoribbons with length of 500–1000 nm. As shown in Fig. 5e, the inset SAED pattern along the [1 $\bar{1}$ 0] zone axis of a nanoribbon indicates that CuO nanopetals are single crystalline. This is corroborated by the HRTEM image (Fig. 5e) of the nanoribbon.

When the molar ratio of NaOH to $Cu(NO_3)_2$ was 40, CuO nanoribbons or nanorods (samples A1–A3) were obtained. The formation mechanism of these CuO 1D structures was investigated. During the reaction process, blue intermediate precipitates occurred first. The blue precipitate was collected during preparation of sample A3. The XRD pattern (Fig. 6a) of it could be indexed to orthorhombic $Cu(OH)_2$ (JCPDS 13-0420). The peaks marked with "*" indicate the existence of a little impurity of CuO. The TEM image in Fig. 6b shows that the blue

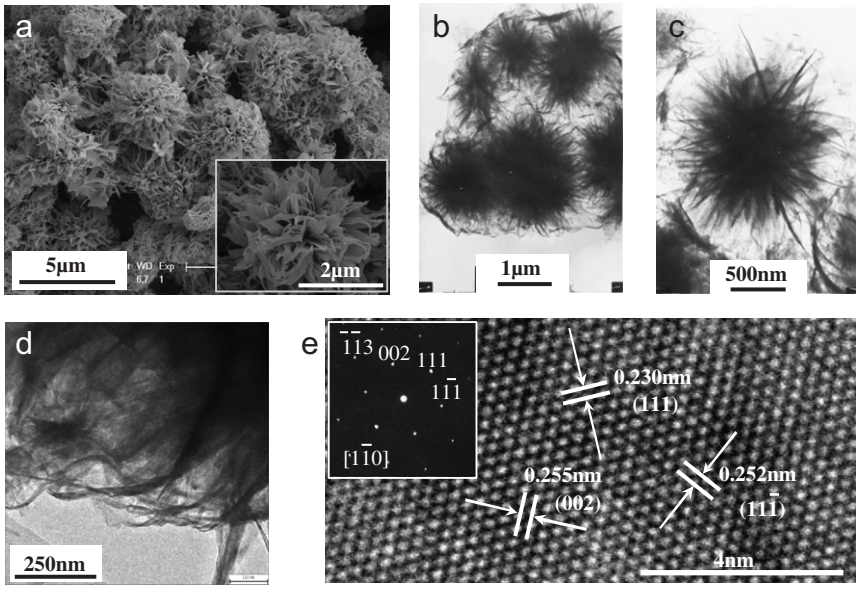

Fig. 5. FE-SEM (a) and TEM (b) images of spherical CuO assemblies corresponding to sample B3; TEM (c, d) images of a single CuO microsphere in it; HRTEM (e) image of a single CuO nanorod in it. Inset of part (a): a higher magnification FE-SEM image of a single CuO microsphere; inset of part (e): SAED pattern of the single CuO nanoribbon.

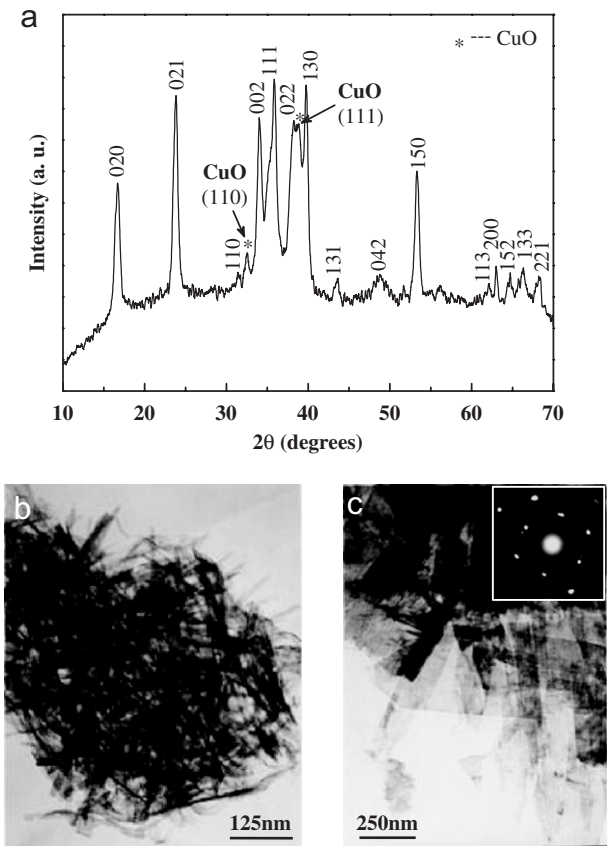

Fig. 6. XRD pattern (a) and TEM image (b) of $Cu(OH)_2$ nanoribbons at room temperature for ~3 min during preparing sample A3; TEM (c) images of CuO nanoplates (sample A3′) at room temperature for 26 h without ethanol as a solvent. Inset of part (c): SAED pattern of a single CuO nanoplate.

intermediate precipitate $Cu(OH)_2$ is composed of large amount of nanoribbons. After the subsequent heating or aging process, the intermediate $Cu(OH)_2$ lost H_2O molecules and was transformed into CuO completely and the precursor $Cu(OH)_2$ nanoribbon structure retained to yield CuO nanoribbons.

The evolution process can be illustrated as following:

$$Cu^{2+} + 2OH^- \rightarrow Cu(OH)_2 \text{ (nanoribbons)}$$
$$\rightarrow CuO \text{ (nanoribbons)} + H_2O.$$

Ethanol was found to play an important role in the synthesis of monodispersed and uniform CuO nanoribbons. A comparative experiment (sample A3′) without ethanol was devised to confirm it. The reagent $Cu(NO_3)_2$ was dissolved in distilled water instead of ethanol and other reaction conditions were kept the same as those for preparing sample A3. Fig. 6c presents typical TEM image of the as-prepared sample A3′, which consists of highly agglomerated nanoplates without uniform morphology, and the corresponding ED pattern indicates that sample A3′ is composed of single-crystalline CuO nanoplates. In comparison with the morphology of sample A3, it can be found that ethanol has great influence on the morphology of the as-prepared CuO sample.

Ethanol could also improve the reaction rate. During the reaction, it was only after ~3 min that the blue solution turned black in the preparation of sample A3 while in the comparison experiment of sample A3′, it was after 5–6 h that the blue solution turned black.

The surface tension of water is 77.82 mN m^{-1} at 20 °C while that of absolute ethanol is 22.39 mN m^{-1} [28]. Since alkalis such as the hydroxides of sodium and potassium raise the surface tension of water [29], the high-concentrated NaOH aqueous solution has even higher surface tension than water. When the $Cu(NO_3)_2$ ethanol solution is dropped into NaOH aqueous solution in the synthesis of samples A1–A3, the surface tension of the NaOH solution is markedly decreased. The nuclei of intermediate product $Cu(OH)_2$ are produced and may be wrapped by surrounding ethanol quickly, thus dispersed much better, and $Cu(OH)_2$ will be easily dehydrated to form fine CuO nanoribbons in a very short time. While the $Cu(NO_3)_2$ aqueous solution is dropped into NaOH aqueous solution, the surface tension of the NaOH solution is still rather high and the intermediate $Cu(OH)_2$ will be greatly agglomerated. Due to large agglomeration of $Cu(OH)_2$ nuclei, it will take a longer time for the intermediate to dehydrate into CuO. Thus, final CuO is much bigger and less uniform than that prepared with $Cu(NO_3)_2$ ethanol solution. Therefore, ethanol not only makes the dehydration of $Cu(OH)_2$ faster, but also makes CuO nanoribbons more uniform and monodispersed.

When the molar ratio of NaOH to $Cu(NO_3)_2$ was increased to 200, the assemblies composed of hundreds of nanoribbons (or nanorods) (samples B1–B3) were obtained. When the $Cu(NO_3)_2$ ethanol solution was slowly added into the high concentration of NaOH aqueous solution, blue intermediate precipitates were not observed as occurring in the synthesis of samples A1–A3; however, a deep blue solution was formed first and finally a black precipitate was formed. The formation mechanism of CuO spherical and flower-like assemblies may be illustrated in Scheme 1. Due to the high concentration of NaOH aqueous solution, $[Cu(OH)_4]^{2-}$ ions are first produced instead of $Cu(OH)_2$ precipitates. Because of the steric effect and hydrophilicity of hydroxyl, $[Cu(OH)_4]^{2-}$ ions may exist in spherical clusters [30]. Then a condensation phenomenon, combined with a loss of two hydroxyl ions and one water molecule, may lead to the formation of CuO [31,32]. Thus, the $[Cu(OH)_4]^{2-}$ clusters are dehydrated and they in situ generate a suitable amount of aggregates comprising of CuO nuclei which act as the seeds for the spherical CuO assemblies. Each nanocluster in the solution has its own orientation and works as a nucleus for further growth [33,34]. These nuclei develop their own preferred growth during the reaction process. Finally, the assemblies composed of hundreds of nanoribbons (or nanorods) (samples B2 and B3) can be prepared.

The process can be expressed as follows:

$Cu^{2+} + 4OH^- \rightarrow [Cu(OH)_4]^{2-} \rightarrow CuO$ (spherical or flower-like assemblies) $+ H_2O + 2OH^-$.

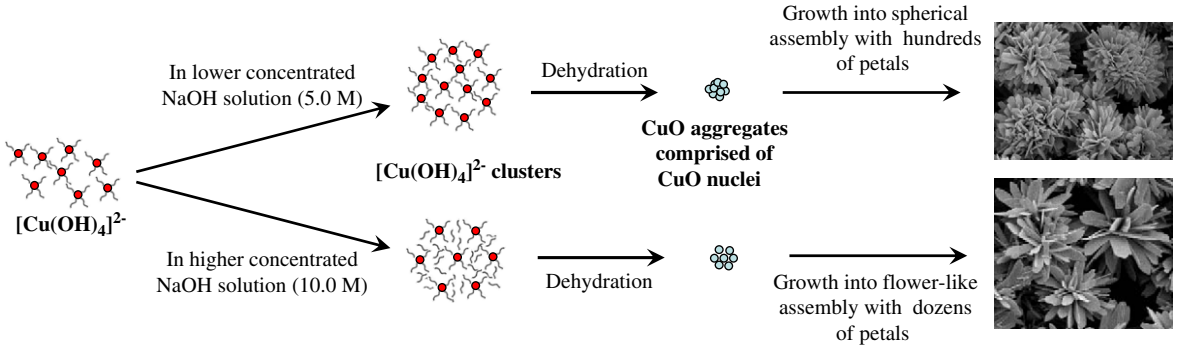

Scheme 1. Illustration of the formation mechanism of spherical and flower-like CuO assemblies from $[Cu(OH)_4]^{2-}$.

When the concentration of the starting NaOH solution was further increased to 10.0 M, which was twice as much as that of NaOH to fabricate CuO spherical assembly (samples B2 and B3), CuO flower-like assembly (sample B1) was obtained. It can be explained that in higher concentration of NaOH, each cluster of $[Cu(OH)_4]^{2-}$ ions is surrounded by more hydroxyl ions, which brings about great steric effects. As a result, the number of the $[Cu(OH)_4]^{2-}$ contained in the cluster is markedly decreased. More hydroxyl groups around the surface of CuO nuclei decrease the packing probability of CuO aggregates. So the $[Cu(OH)_4]^{2-}$ clusters are dehydrated to form CuO flower-like assemblies which contain fewer nanorods than those of the CuO microsphere of sample B2.

UV–vis spectrophotometry is used to characterize the optical absorption properties of the obtained CuO samples. For measurements, the CuO products are dispersed in absolute ethanol by ultrasonication. It is reported that not only the size but also the morphology and crystallinity of nanocrystals would affect the optical absorption peak [35–37], which is also confirmed by our experiment. The UV–vis spectra of the CuO products exhibit weak broad absorption peaks in the 400–600 nm range (shown in Fig. 7). The CuO nanorods prepared at 100 °C (sample A1) show a band position at ~444 nm (Fig. 7a). The CuO nanoribbons prepared at 50 °C (sample A2) show a band position at ~438 nm (Fig. 7b). When the reaction temperature decreases to room temperature, the obtained nanoribbons (sample A3) exhibit an absorption peak at ~436 nm. The difference of the absorption peaks for samples A1–A3 may result from their difference in crystal size and crystallinity. It has been reported that the increase in crystal size and the improvement of crystallization result in red-shift [36]. Consistent with the reports that the absorption peak red-shifts when the building blocks aggregate into assemblies which will result in larger size [10,35], all the CuO assemblies (samples B1–B3) produce red-shifts in absorption peaks compared with samples A1–A3. The optical absorption peak of the CuO microspheres built from hundreds of nanorods (sample B2) red-shifts to ~566 nm (Fig. 7d). As for sample B1, the absorption peak is centered at ~551 nm (Fig. 7e), maybe owing to a decrease in the number of the nanorods from

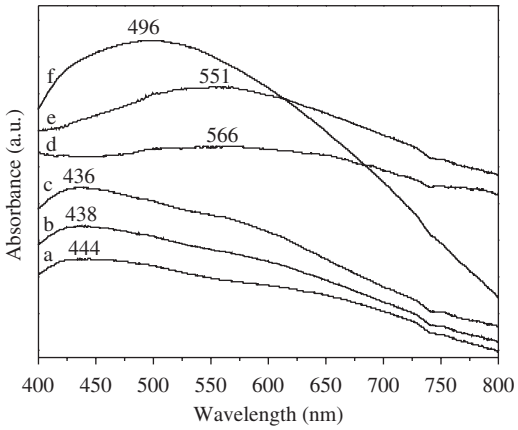

Fig. 7. UV–vis absorption spectra of the as-prepared CuO products: (a) CuO nanorods prepared at 100 °C (sample A1); (b) CuO nanoribbons prepared at 50 °C (sample A2); (c) CuO nanoribbons prepared at room temperature (sample A3); (d) CuO spherical assemblies prepared at 100 °C (sample B2); (e) CuO flower-like assemblies prepared at 100 °C (sample B1) and (f) CuO spherical assemblies prepared at room temperature (sample B3).

which the flower-like assembles are built. The absorption peak of the CuO microspheres prepared at room temperature (sample B3) is centered at ~496 nm (Fig. 7f). It can be seen that the red-shift in absorption peak for sample B3 is not as big as those for samples B1 and B2, probably due to its smaller assembly size as well as smaller building blocks.

4. Conclusion

In summary, CuO nanoribbons or nanorods and their assembly into hierarchical structures have been synthesized, respectively, by a simple solution route. The morphologies and crystallization of the as-prepared CuO were mainly determined by the molar ratio of NaOH to $Cu(NO_3)_2$, reaction temperature and the concentration of the starting NaOH solution. One-dimensional CuO nanoribbons or nanorods were prepared with the molar ratio of NaOH to $Cu(NO_3)_2$ of 40. When the molar ratio of NaOH to $Cu(NO_3)_2$ was increased to 200, spherical or flower-like hierarchical assemblies which were built with 1D CuO nanoribbons or nanorods were synthesized. Ethanol

greatly influences the morphologies of CuO and can enhance the dehydration rate of $Cu(OH)_2$ by reducing the surface tension of the solution. This synthetic method is very simple and mild and is able to control the morphology of the nanostructure effectively. We hope that this simple synthetic route can be extended to other systems involving metal complexes with suitable combination of metals and ligands. Such different morphologies of CuO nanomaterials would be expected to have some potential applications in optical electronic devices.

Acknowledgments

This project was financially supported by the National Natural Science Foundation of China (NSFC nos. 20301005 and 20576024), International Cooperation Project of Science and Technology of Anhui Province (04088012) and the Excellent Young Teachers Program of the Ministry of Education of China.

References

[1] A.Q. Musa, T. Akomolafe, M.J. Carter, Sol. Energy Mater. Sol. Cells 51 (1998) 305.
[2] J.B. Reitz, E.I. Solomon, J. Am. Chem. Soc. 120 (1998) 11467.
[3] H. Wang, J.Z. Xu, J.J. Zhu, H.Y. Chen, J. Cryst. Growth 244 (2002) 88.
[4] W. Wang, Y. Zhan, X. Wang, Y. Liu, C. Zheng, G. Wang, Mater. Res. Bull. 37 (2002) 1093.
[5] M.K. Wu, J.R. Ashburn, C.J. Torng, P.H. Hor, R.L. Meng, L. Gao, Z.J. Huang, Y.Q. Wang, C.W. Chu, Phys. Rev. Lett. 58 (1987) 908.
[6] X.G. Zheng, C.N. Xu, Y. Tomokiyo, E. Tanaka, H. Yamada, Y. Soejima, Phys. Rev. Lett. 85 (2000) 5170.
[7] D. Prabhakaran, C. Subramanian, S. Balakumar, P. Ramasamy, Physica C 319 (1999) 99.
[8] K. Borgohain, S.J. Mahamuni, Mater. Res. 17 (2002) 1220.
[9] P. Poizot, S. Laruelle, S. Grugeon, L. Dupont, J.M. Taracon, Nature 407 (2000) 496.
[10] J.T. Zhang, J.F. Liu, Q. Peng, X. Wang, Y.D. Li, Chem. Mater. 18 (2006) 867.
[11] A.H. MacDonald, Nature 414 (2001) 409.
[12] R.V. Kumar, Y. Diamant, A. Gedanken, Chem. Mater. 12 (2000) 2301.
[13] F. Lanza, R. Feduzi, J.J. Fuger, Mater. Res. 5 (1990) 1739.
[14] X.P. Gao, J.L. Bao, G.L. Pan, H.Y. Zhu, P.X. Huang, F. Wu, D.Y. Song, J. Phys. Chem. B 108 (2004) 5547.
[15] T. Maruyama, Sol. Energy Mater. Sol. Cells 56 (1998) 85.
[16] A.E. Rakhshni, Solid State Electron. 29 (1986) 7.
[17] S. Iijima, Nature 354 (1991) 56.
[18] F. Favier, E.C. Walter, M.P. Zach, T. Benter, R.M. Penner, Science 293 (2001) 2227.
[19] Y.W. Cao, R. Jin, C.A. Mirkin, J. Am. Chem. Soc. 123 (2001) 7961.
[20] M.H. Cao, C.W. Hu, Y.H. Wang, Y.H. Guo, C.X. Guo, E.B. Wang, Chem. Commun. (2003) 1884.
[21] X.C. Jiang, T. Herricks, Y.N. Xia, Nano Lett. 2 (2002) 1333.
[22] Y. Chang, H.C. Zeng, Cryst. Growth Des. 4 (2004) 397.
[23] B. Liu, H.C. Zeng, J. Am. Chem. Soc. 126 (2004) 8124.
[24] Y.Y. Xu, D.R. Chen, X.L. Jiao, J. Phys. Chem. B 109 (2005) 13561.
[25] W.X. Zhang, S.X. Ding, Z.H. Yang, A.P. Liu, Y.T. Qian, S.P. Tang, S.H. Yang, J. Cryst. Growth 291 (2006) 479.
[26] C.L. Zhu, C.N. Chen, L.Y. Hao, Y. Hu, Z.Y. Chen, J. Cryst. Growth 263 (2004) 473.
[27] X.G. Wen, W.X. Zhang, S.H. Yang, Langmuir 19 (2003) 5898.
[28] J.A. Dean, Lange's Hand Book of Chemistry, 15th ed., McGraw-Hill, New York, 1999, pp. 90–134 (Section. 5).
[29] J.J. Bikerman, Surface Chemistry, second ed., New York, 1958, p. 76.
[30] H. Cölfen, S. Mann, Angew. Chem. Int. Ed. 42 (2003) 2350.
[31] G.H. Du, G.V. Tendeloo, Chem. Phys. Lett. 393 (2004) 64.
[32] Y. Cudennec, A. Lecerf, Solid State Sci. 5 (2003) 1471.
[33] J. Jiang, S.H. Yu, W.T. Yao, H. Ge, G.Z. Zhang, Chem. Mater. 17 (2005) 6094.
[34] A.L. Pan, R.C. Yu, S.S. Xie, Z.B. Zhang, C.Q. Jin, B.S. Zou, J. Cryst. Growth 282 (2005) 165.
[35] C.H. Lu, L.M. Qi, J.H. Yang, X.Y. Wang, D.Y. Zhang, J.L. Xie, J.M. Ma, Adv. Mater. 17 (2005) 2562.
[36] H.R. Zhang, C.M. Shen, S.T. Chen, Z.H. Xu, F.S. Liu, J.Q. Li, H.J. Gao, Nanotechnology 16 (2005) 267.
[37] J.P. Yang, F.C. Meldrum, J.H. Fendler, J. Phys. Chem. 99 (1995) 5500.